# Onia production at ATLAS

*Takashi Matsushita, on behalf of the ATLAS Collaboration*
*Organization of Advanced Science and Technology, Kobe University, Kobe, JAPAN*

## 1 Introduction

The ATLAS detector [1] is a multipurpose particle physics apparatus built at the Large Hadron Collider (LHC). In addition to a wide range of measurements of high mass particles produced at high transverse momenta ($p_T$), both within or beyond the Standard Model, ATLAS has a rich quarkonium physics programme concentrating on low-$p_T$ di-muon final states. Quarkonia are formed from a quark-antiquark pair of the same flavour. Despite being among the most studied of the bound-quark systems, there is still no clear understanding of the production mechanisms that can consistently explain both the cross-section and spin-alignment measurements [2]. The LHC provides the opportunity to test existing models at a higher energy regime, a higher $p_T$ and a wider rapidity ranges than previously.

## 2 Quarkonia production and observation of $\chi_b$(3P)

In order to allow efficient collection of low-$p_T$ di-muon samples, dedicated $b$-physics triggers had been developed. Two low-$p_T$ muons identified by hardware-based first level trigger are subsequently analysed by higher level software trigger algorithms. Once the muons are confirmed, a fit is performed to the combined vertex and mass constraints are applied. Figure 1 shows the di-muon mass spectrum for events recorded in the first half of 2011 data taking period. The coloured histograms show the significant data samples collected by the dedicated $b$-physics triggers. In 2010 and 2011, ATLAS has recorded 48 pb$^{-1}$ and 5.6 fb$^{-1}$ of data, respectively, from $pp$ collisions at a centre of mass energy of 7 TeV.

ATLAS has measured the differential cross-sections of inclusive, prompt and non-prompt $J/\psi$ production using 2.2 pb$^{-1}$ of 2010 data [4]. Trigger and reconstruction efficiencies were measured in data and validated with Monte Carlo simulations. Weights incorporating acceptance and efficiency corrections were applied to quarkonia candidates on an event-by-event basis before fits were used to extract cross-section. $J/\psi$ can be produced either promptly from the hard interaction or non-promptly via decay of a $b$-hadron. $J/\psi$ from $B$-decays have positive displaced di-muon vertices and can be distinguished from the prompt production via the pseudo-proper time discriminant,

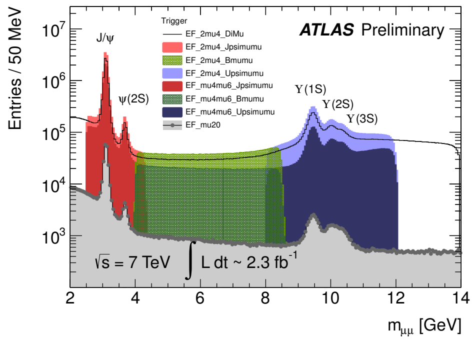


Figure 1: Invariant mass of oppositely charged muon candidate pairs selected by a variety of ATLAS triggers. The coloured histograms show events selected by the dedicated $b$-physics triggers compared to those triggered by the single muon trigger (grey). The different colours correspond to triggers with different mass ranges [3].

$\tau = L_{xy} \cdot m_{\mathrm{PDG}}^{J/\psi}/p_T^{J/\psi}$, where $L_{xy}$ is the transverse decay length of the $J/\psi$ vertex. Figure 2 shows the inclusive $J/\psi$ cross-section as a function of the $p_T^{J/\psi}$ for one rapidity bin (left) and the $\tau$ distribution (right). By combining these two measurements, the prompt and non-prompt $J/\psi$ cross-sections were derived. The largest source of systematic uncertainty of the cross-section measurement is due to the unknown spin alignment of the $J/\psi$. Five spin alignment scenarios were identified that induce the largest envelope of variation on visible cross-sections. Figure 3 shows the non-prompt (left) and prompt (right) $J/\psi$ production cross-sections as a function of $p_T^{J/\psi}$ compared to theoretical predictions. The measured non-prompt cross-section is in good agreement with Fixed-Order Next-to-Leading-Log theoretical predictions. The prompt cross-section is compared to colour-singlet model (CSM) NLO and NNLO$^*$ pQCD predictions and to the phenomenological Colour Evaporation Model (CEM). The CEM predictions describe the shape better and the NNLO$^*$ prediction shows a significant improvement in the normalisation over the NLO prediction.

Production cross-sections of $\Upsilon$(1S) have been derived in bins of rapidity and $p_T^{\Upsilon(1S)}$ with 1.1 pb$^{-1}$ of 2010 data [5]. The measurement was restricted to the fiducial region, $p_T^\mu > 4$ GeV and $|\eta^\mu| < 2.5$, to remove the uncertainty due to the spin alignment. Unfolded differential cross-sections are compared to CSM NLO prediction in figure 4 left and significant disagreement is observed. However, the prediction does not include feed-down from higher mass states estimated to contribute a factor of two at the Tevatron [6].

ATLAS observed a new $\chi_b$(3P) state through its radiative decays to $\Upsilon$(1S) and $\Upsilon$(2S) with 4.4 fb$^{-1}$ of data collected in 2011 [7]. Radiative decays of $\chi_b$(3P) have been reconstructed from the photon emitted during the transition, and the subsequent decay of the $\Upsilon$ into two muons. Figure 4 right shows the mass distribution

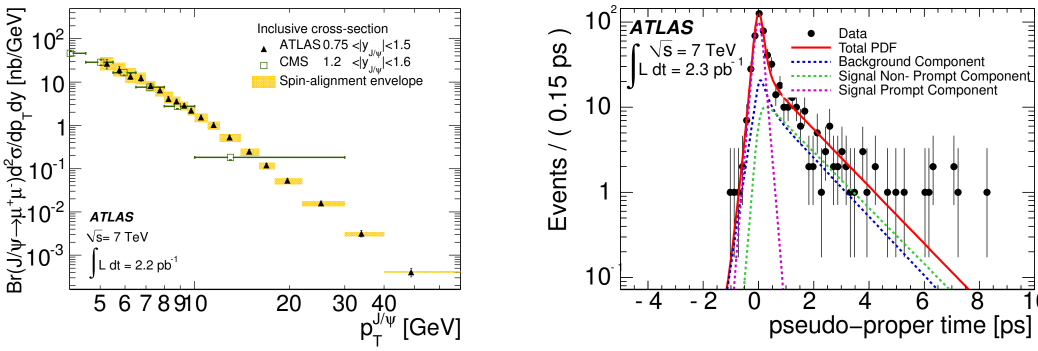


Figure 2: Left figure shows inclusive $J/\psi$ production cross-section as a function of $p_T^{J/\psi}$ in 0.75< $|y|$ <1.5 rapidity bin. Right figure shows $\tau$ distribution of $J/\psi$ candidates for a selected $p_T$ bin ($9.5 < p_T < 10.0$ GeV) in the $|y| < 0.75$ rapidity bin. The points are data and the solid line is the result of the unbinned maximum likelihood fit [4].

for candidates with converted photons. The mass for $\chi_b$(3P) is determined as 10.539 $\pm$ 0.005 (stat.) $\pm$ 0.009 (syst.) GeV, which is consistent with the expectation from theoretical models averaging the mass over the three $\chi_b$(3P) hyperfine triplet states.

# 3 Summary

The ATLAS quarkonia programme has produced many important measurements of production cross-sections which are already providing valuable input for theoretical models. A new bottomonium state, $\chi_b$(3P), has been observed for the first time.

# References


[1] ATLAS Collaboration, *JINST* **3**, S08003 (2008)

[2] N. Brambilla *et al.*, CERN Yellow Report, CERN-2005-005, 2005;
N. Brambilla *et al. Eur. Phys. J.* C **71**, 1534 (2011)

[3] ATLAS Collaboration, `https://twiki.cern.ch/twiki/bin/view/AtlasPublic/BPhysPublicResults`

[4] ATLAS Collaboration, *Nucl. Phys.* B **850**, 387 (2011)

[5] ATLAS Collaboration, *Phys. Lett.* B **705**, 9 (2011)

[6] P. Artoisenet *et al.*, *Phys. Rev. Lett.* **101**, 152001 (2008)

[7] ATLAS Collaboration, *Phys. Rev. Lett.* **108**, 152001 (2012)

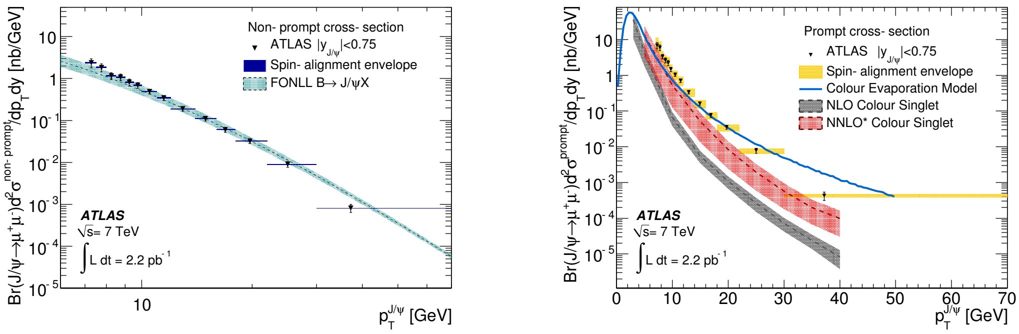


Figure 3: Non-prompt (left) and prompt (right) $J/\psi$ production cross-sections as a function of $p_T^{J/\psi}$. The non-prompt (prompt) cross-section is compared to predictions from FONLL (NLO, NNLO$^*$ and the CEM). Coloured bands show the changes of the results under spin-alignment scenarios representing a theoretical uncertainty [4].

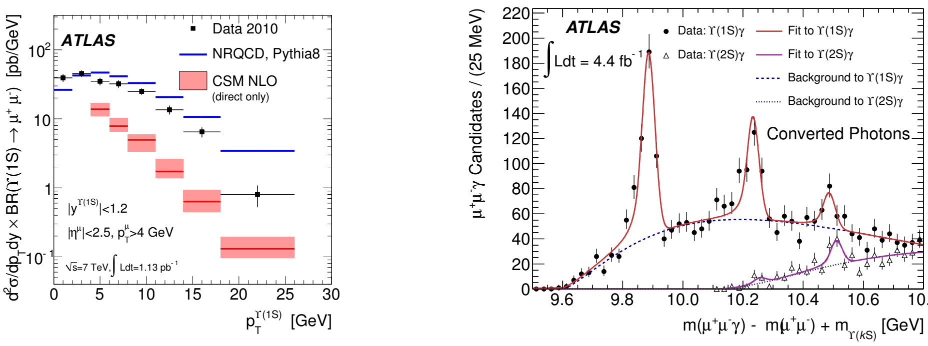


Figure 4: Left figure shows $\Upsilon(1\mathrm{S})$ cross-section for $|y^{\Upsilon(1\mathrm{S})}| < 1.2$ as a function of $p_T^{\Upsilon(1\mathrm{S})}$. Also shown is the CSM and the NRQCD predictions. Right figure shows the mass distribution of $\chi_b \to \Upsilon(k\mathrm{S})\gamma$ $(k = 1, 2)$ candidates for converted photons. $\chi_b \to \Upsilon(1\mathrm{S})\gamma$ and $\chi_b \to \Upsilon(2\mathrm{S})\gamma$ decays are plotted using circles and triangles, respectively. Solid (dashed) lines show the total (background) fit result for each mass window [5, 7]